

Dipolar-Modulated Charge-Doped Trilayer Organic Semiconductor n–n Heterojunction

Jianing Liu,* Katharina Ditte, Wei Jiang, Zhaohui Wang, and Cornelia Denz*

Since n–n heterojunction theory was put forward in the 1950s,^[1] it has been considered very useful for modeling one-side-modulation-doped field-effect high-mobility electron transistors (HMETs) and single/double quantum wells, as well as investigating 2D electron gas (2DEG) in solid-state physics.^[2] In general, an n–n heterojunction consisting of two n-type semiconductors with different Fermi levels, forms electron accumulation/depletion regions at either side of the heterojunction. Charge transport is dominated by majority carriers (electrons) and requires a potential barrier to confine minority carriers into a small active region in order to effectively reduce the diffusion length of these minority carriers.^[3] The main difficulty in the operation of an organic (opto)electronic device is efficient charge injection from an electrode,^[4] so to reduce contact resistance at interfaces and to achieve a desired band-offset is nontrivial.^[5] Another hurdle involves the design of efficient organic (opto)electronic devices, in which an organic donor–acceptor (D–A) interface plays a crucial role in the charge generation and separation processes. Conventionally, a D–A interface is viewed as occurring at a p–n heterojunction.^[6] Indeed, if and when a D–A interface with an induced density of interfacial states can be achieved at an n–n heterojunction by techniques such as impurity- and dipolar-modulated charge-doping, it could be used as an alternative to explore novel (opto)electronic devices with extensive material combination and new functional properties, for example, a switchable, bidirectional photo/electric-current flow instead the unidirectional flow in a p–n heterojunction. Of course, a problem of the commonly used impurity charge-doping that has persisted is the nontunability of the doping charge density. Surface modification by dipoles occurring on an atomic length scale in the neighborhood of the interface has proven very successful in introducing changes in the interfacial composition and structure, modifying band-offset, and improving charge transport.^[7,8]

Therefore, polar surface modification or dipolar-modulated charge-doping with a tunable doping charge density, rather than the usual impurity doping, is expected to facilitate the fabrication of efficient n–n heterojunctions.^[3]

From this perspective, we developed here a dipolar-modulated charge-doped trilayer organic semiconductor n–n heterojunction (**Scheme 1**), a trilayer configuration constructed by layer-by-layer (LBL) spin-coating of polar electret hydrogel poly(vinyl alcohol) (PVA), n-type semiconductor fullerene derivative phenyl-C₆₁-butyric acid methyl ester (PCBM), and self-synthesized, air-stable n-type semiconductor perylene bisimide (PBI) onto an indium tin oxide (ITO) electrode. Its thickness and in-plane dimensions are: PVA (≈500–600 nm, ≈2 mm × 2 mm), PCBM (≈10–20 nm, ≈2 mm × 2 mm), PBI (≈30–100 nm, ≈2 mm × 2 mm) (see Supporting Information (SI), Figure S1–S3).

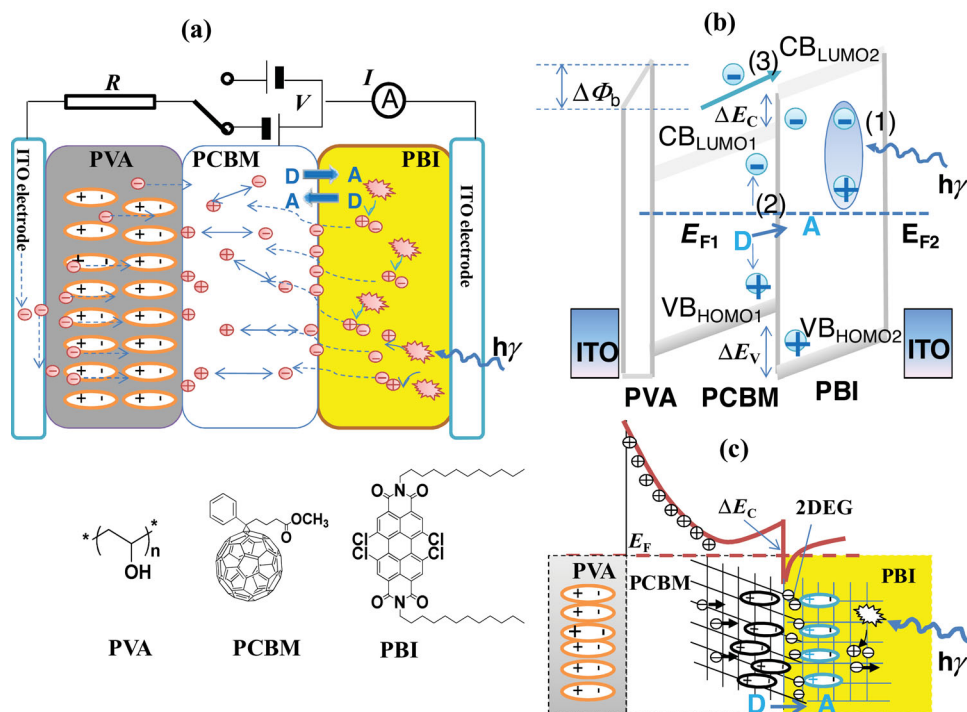
In the trilayer configuration, an important function of PBI is to generate excitons (charge pairs) due to its ability to absorb and harvest visible light (SI, Figure S4). PCBM is mainly used to carry out both charge separation through D–A interface^[9] and carrier transport, owing to its relatively high mobility of electrons and holes (ambipolar transport characteristics).^[10–11] However, neither PBI nor PCBM single layers are suitable to be directly applied in efficient (opto)electronics due to the domination of hole–electron recombination.^[12] A two-layer combination of PBI/PCBM was then used to construct an n–n heterojunction. For establishing a band discontinuity with the desired barrier height in an n–n heterojunction, an abrupt interface through LBL instead of bulk blending is necessary, as demonstrated previously^[13] and verified by a contrast optoelectronic experiment of PBI and PCBM bulk-blending (SI, Figure S5). Even so, to get an optoelectronic response of the PBI/PCBM bilayer through LBL growth is still operationally difficult (SI, Figure S6B,C). This could be attributed to four main factors: 1) the extrinsic defects and disorder or traps in PCBM films considerably mask charge transport in organic materials and lead to an increase in contact resistance at the interface close to the ITO electrode.^[14] 2) The large population of intrinsic electrons near the Fermi level of the ITO electrode far exceeds that of photoelectrons, so the output optoelectronic signal is annihilated in the dark current. 3) Oxidation degradation and thermal instability are both issues for n-type organic semiconductor PCBM.^[15] 4) The lowest occupied molecule orbital (LUMO) level and highest occupied molecule orbital (HOMO) levels between PBI and PCBM are almost equal (LUMO: 3.6 eV/3.75 eV and HOMO: 6.15 eV/6.1 eV; see SI, Figure S6B,C).^[16,17] In order to tune the conduction band

Dr. J. Liu, K. Ditte, Dr. C. Denz
Institut für Angewandte Physik
Westfälische Wilhelms-Universität Münster
48149, Münster, Germany
E-mail: Jianing.Liu@tu-braunschweig.de;
denz@uni-muenster.de



Dr. W. Jiang, Dr. Z. Wang
Beijing National Laboratory for Molecular Sciences
Institute of Chemistry
Chinese, Academy of Sciences, 100190 Beijing, China

DOI: 10.1002/sml.201101776



Scheme 1. a) Schematic illustration of PBI/PCBM/PVA trilayer n-n heterojunction with switchable bidirectional electron flow and organic molecular structures. Corresponding to bias, the dipolar direction of PVA and polar-modulated charge-doping can be tuned. An efficient bidirectional electronic transport is then introduced, which is functionally similar to a switch between donor and acceptor at the n-n interface. b) Dipole-induced barrier $\Delta\Phi_b$, conduction and valence band discontinuities ΔE_C and ΔE_V at the PBI/PCBM n-n interface. The three steps for generation of photocurrent are labelled: exciton generation (1), charge separation (2), and transport (3). c) Sketch of band-bending and charge trapping at PCBM/PVA and PBI/PCBM interfaces, the dipolar-modulation induced 2DEG at the PBI/PCBM n-n interface, molecular dipolar alignment, and the major charge (electron) transport from D→A. Also see SI, Figure S6A,B and Figure S9.

discontinuity (ΔE_C) and suppress the unfavorable factors, deposition of a polar electret material on the electrode surface should be a suitable approach.^[18] The role of the local dipoles generated in the interface region has been highlighted in a variety of theoretical and experimental works,^[19] where a charge-injection barrier can be created at the electrode/organic interface. In general, the barrier height ($\Delta\Phi_b$) is given by $\Delta\Phi_b = 4\pi\delta$, where δ is the surface dipole density.^[20] Clearly, the band alignment can be tuned by applying an electric field bias that leads to changes in δ . Furthermore, the large dipole density occurring at the interface pinning to the Fermi level will introduce an abrupt change of surface states (SI, Figure S6A).

Conventionally, PVA, a semicrystalline polar hydrogel material, usually serves as the dielectric insulator due to its large optical bandgap (4.84–5.44 eV).^[21] However, its ionic conductivity can be tailored by thermally generated carriers, suitable dopant materials, or γ -radiation, altering the physical properties of PVA and/or the host matrix.^[22–25] It seems reasonable to expect that the conductivity of PVA could be also tailored by attaching photoactive organic semiconductor layers onto it. In our optoelectronic experiment, the photoinduced conductivity and piezoelectricity have been discovered in the LBL constructions of PVA and photoactive organic semiconductors (SI, Figure S8), whereas pure PVA did not exhibit such behavior (SI, Figure S7). On the other hand, we noted that PVA as an electret material, that

has quasi-permanent charge storage or dipole polarization due to rich hydroxyl (OH^-) groups,^[26] promises tunable polarity, governing transport and accumulation of charge carriers at the contact interface. Here, PVA in contact with PCBM tends to modify the semiconductor band lineup or conduction band discontinuity (ΔE_C) by dipolar-modulated charge-doping at the PCBM/PVA interface, which plays an important role in the PBI/PCBM/PVA trilayer n-n heterojunction in terms of orienting permanent dipoles, trapping charges near the heterogeneous grain boundaries (Scheme 1c). On the grounds of the ambipolar transport nature of PCBM,^[10–11] the redistribution of charge density at the PBI/PCBM n-n heterojunction brings about a new band discontinuity by means of polar modification. The band discontinuity will be approximately determined by lining up the ‘charge neutrality level’. When the levels are not aligned, charges would flow between the two materials (Scheme 1a–c). As shown in Scheme 1a, there exists a substantial bidirectional control of electron transport in an n-n heterojunction, different to the unidirectional transport in a p-n heterojunction. Corresponding to reversing the bias between $-V$ and $+V$, the energy band structure between the accumulation and depletion regions of majority carriers (electrons) at the PBI/PCBM n-n interface, along with the reversible direction of system polarity, can be transformed, leading to an alteration of the density of interfacial states functionally similar to the transformation between donor and acceptor (Scheme 1c

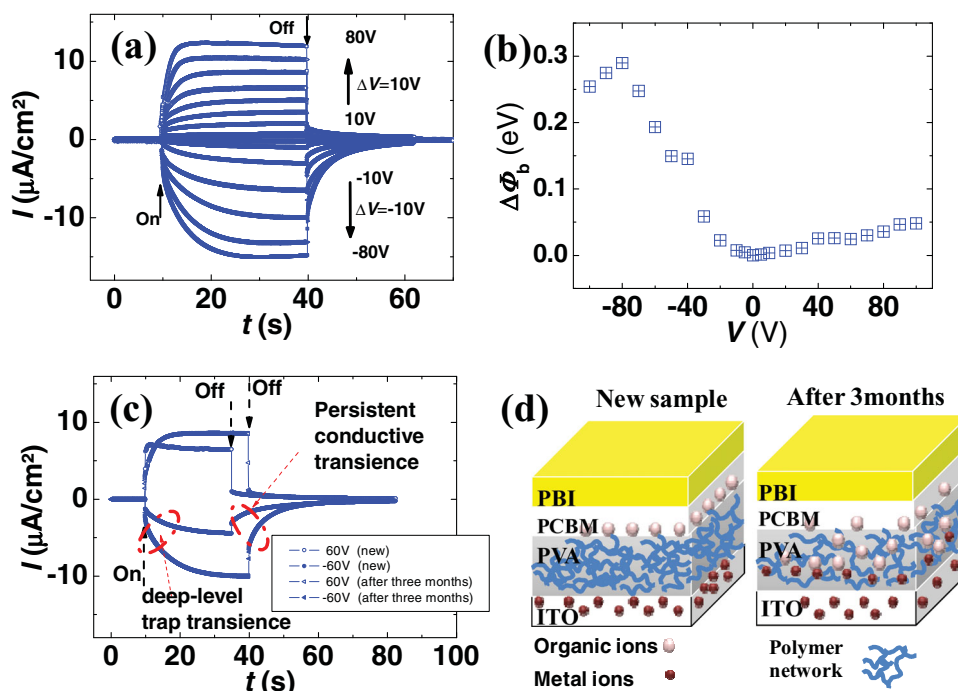


Figure 1. a) The time-dependent photocurrent features under bidirectional bias control. b) The bias-dependent dipolar barrier height $\Delta\Phi_b$. Due to charge offset by OH^- groups at PVA surface, the dipolar barrier $\Delta\Phi_b$ induced by $+V$ is lower than that by $-V$. c, d) I - t plot and schematic illustration of the time-dependent changes to the PVA layer, comparing freshly prepared and 3-month-preserved samples.

and SI, Figure S9). In other words, as PCBM is charge-doped by means of dipolar modulation, the PBI/PCBM n-n junction is transformed into an n-n⁺ junction or an n-n⁻ junction (n⁺, n⁻ represent PCBM doped by opposite charges). In principle, the bidirectional control mechanism of the photocurrent can be explained according to self-consistent theory,^[16] and the systematic changes to the bidirectional photocurrent at different biases of $-V$ and $+V$ is illustrated in **Figure 1a**. In addition, due to band-bending at $-V$, some of the photo-generated holes and electrons are confined by an approximately triangular potential near the PCBM/PVA and PBI/PCBM interfaces, respectively, and form a 2DEG at PBI/PCBM interface (Scheme 1c). It should be noted that the dipolar barrier ($\Delta\Phi_b$), bias-tunable via PVA-surface injection (Figure 1b), dominates the molecular dipole across the PCBM, which in turn controls the 2DEG density at the PBI/PCBM interface (Scheme 1c and SI, Figure S9). Such properties make the PBI/PCBM/PVA n-n heterojunction very attractive for HMETs.

It can be seen in Figure 1c that the initial macroscopic transient delay to constant photocurrent density I takes several tens of seconds (time t) after the laser is switched on under $-V$. In fact, the time scale of the transient delay is closely related to the structures of the different materials, for example poly(phenylene vinylene) (microseconds),^[27] pentacene (several tens of seconds)^[28] and semi-insulator GaAs at low temperature (a few hundreds of seconds).^[29] This is thought to be mainly due to the impact of deep-level trapping on the free-carriers. In our experiment, we found that preserving samples at room-temperature was a partial solution to the trapping impact, particularly improving the

photocurrent density compared with freshly prepared samples (Figure 1c). It is shown that, by long-time annealing (3 months) in air at room temperature, PVA absorbs moisture and forms swollen polymer networks, which can be easily permeated by metal and organic ions from ITO electrodes and PCBM layers (Figure 1d). In that way, the ionic conductivity of PVA layer was improved,^[30] which implies also that PVA can, to some extent, protect photoactive semiconductors against degradation caused by oxidation, thermal decomposition or photopolymerization under strong laser illumination, and diffused metal ions. As to the observed transient delay of I under $-V$ after the laser is switched off (Figure 1c), it is a favorable optoelectronic phenomenon termed 'persistent photoconductivity', which is usually found in inorganic materials at low temperature^[31] and occasionally in organics.^[32] Such persistent photoconductivity denotes the presence of a degenerate 2DEG. More interestingly, associated with the intrinsic polarity of the trilayer n-n heterojunction, photocurrent at zero bias can also be induced (**Figure 2a**). Correspondingly, the sum of free transported charge density and released charge density (ΔQ) by 2DEG can be derived from Figure 2a according to $|\Delta Q| = \int |I| dt$ (Figure 2b), in which the former $|\Delta Q| = 2.16 \times 10^{11} \text{ e cm}^{-2}$ from 0 to 30 s under illumination, and the latter $|\Delta Q| = 2.83 \times 10^{10} \text{ e cm}^{-2}$ from 0 to 10 s in the dark. This substantial zero-bias optoelectronic phenomenon indicates the possibility of constructing a photodetector or memory device driven by the optic field alone, revealing that the conductivity and piezoelectric behavior of PVA results from the trapping of photoinduced charge carriers in photoactive semiconductor layers. These results neither follow standard

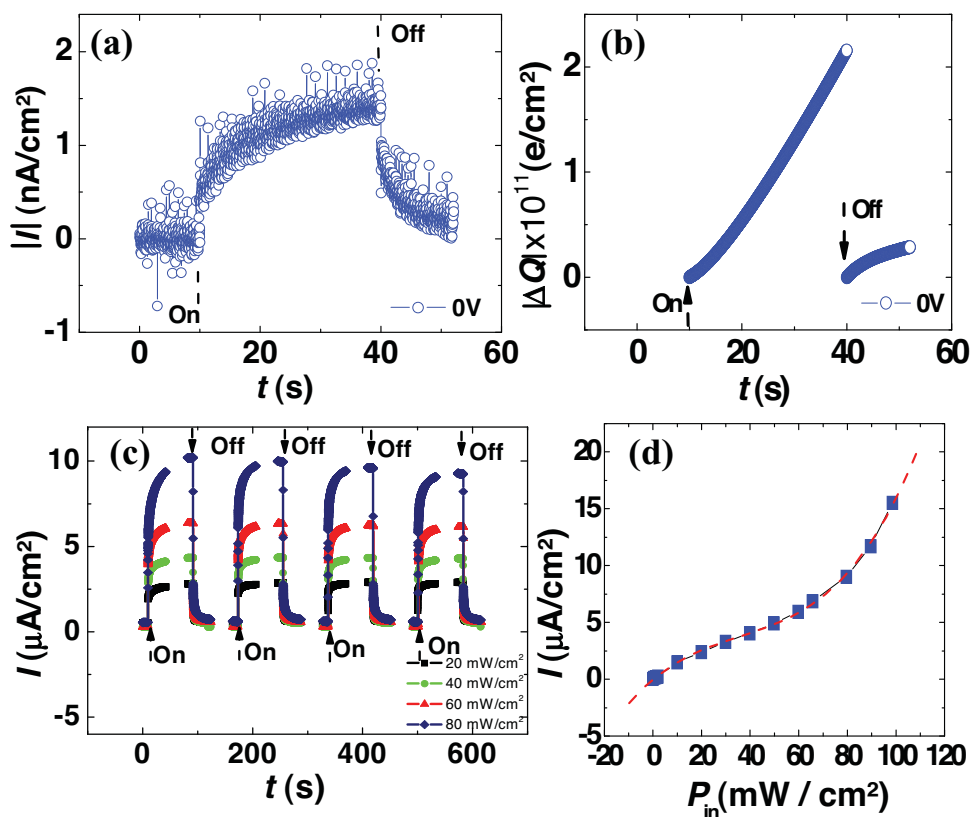


Figure 2. a,b) $|I|$ - t and $|\Delta Q|$ - t plot under zero bias, respectively. c) The energy renewable I - t plot with the laser on and off at 100 V under different light intensities: 20 (■), 40 (●), 60 (▲), and 80 (◆) mW cm^{-2} . d) The nonlinear I - P_{in} plot (■) and third-order polynomial fitting (---): $I = -2.256 \times 10^{-2} + 1.787 \times 10^{-1} P_{\text{in}} - 3.070 \times 10^{-3} P_{\text{in}}^2 + 2.870 \times 10^{-5} P_{\text{in}}^3$, with determination coefficient 0.999.

thermionic emission theory, nor obey tunneling through a simple potential barrier: there is no complete analytic theory except for a hybrid mechanism of the Poole-Frenkel effect and the ionic conductive mechanism.^[4,33–35]

In order to evaluate the reliability of the designed configuration, we have carried out optoelectronic experiments with the laser on and off at a constant bias and different incident laser intensities P_{in} (Figure 2c). The stable photocurrent density I versus P_{in} shown in Figure 2d is found to closely fit the third-order polynomial relation. The same phenomenon is also observed in other PVA-coupled configurations (SI, Figure S10). It can be therefore concluded that the coupled polar dielectric layer PVA highly supports the thermal and mechanical stability of the trilayer and makes it possible to display energy renewable optoelectronic features.

To better understand the function of organic n-n heterojunction in optoelectronic response, it is important to investigate the difference between the PBI/PCBM/PVA trilayer n-n heterojunction and PBI/PVA bilayer without n-n heterojunction. Firstly, I - V characteristic of the trilayer is asymmetric for voltage sweeping in both directions (Figure 3c, SI, Figure S11), while that of the bilayer is symmetric and Ohmic (Figure 3a–c). This shows that the rectifying mechanism of the trilayer is analogous to the rectifying and inverse-rectifying characteristics from n-p

and p-n heterojunctions, respectively. Secondly, the photocurrent density of the trilayer is increased up to three orders of magnitude greater than that of bilayer, which is in accord with the charge-separation functions of the donor/acceptor at a p-n heterojunction.^[6] Furthermore it needs not to worry about the reverse bias breakdown, which generally occurs in single p-n heterojunctions. Experimentally, we underline that organic-based approaches do not rely on conventional single p-n heterojunctions for their functions, but are based upon charge separation at a D-A interface.^[36]

In the trilayer architecture the photocurrent behaves like a leakage current in a field-effect transistor (FET), so the drawback for traditionally using polar polymers as gates^[37] indeed becomes the merit of the heterojunction, in which it either lacks a field-driven channel for energy dissipation or provides a path to make use of the dissipated energy in combination with FETs. It is important to stress, once again, that dipolar-modulated charge-doping is an efficient approach to control charge injection and then band discontinuity, which will enable more organic materials to be used for the design of novel organic (opto)electronic devices by means of a simple deposition process. We expect that what may be viewed as technological hurdles should, in fact, lead to a new approach to an n-n heterojunction and extensive application of polar materials in organic (opto)electronics.

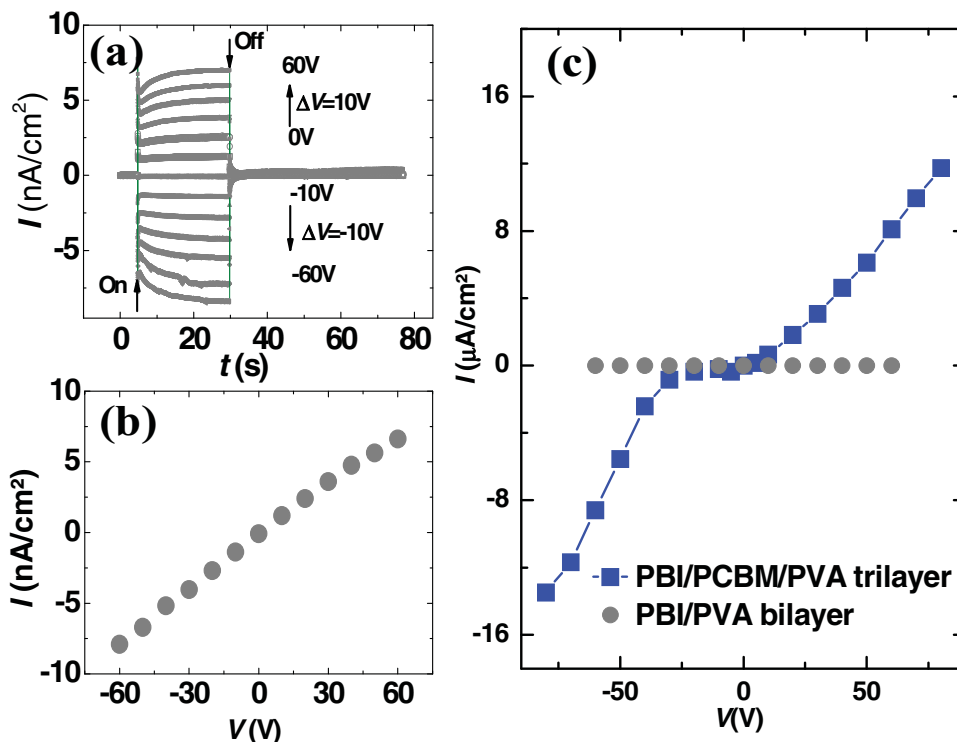


Figure 3. a) I - t and b) I - V plot of PBI/PVA bilayer. c) Comparison of I - V plots between PBI/PCBM/PVA trilayer and PBI/PVA bilayer.

Experimental Section

Material: PVA (87–89% hydrolyzation, MW \approx 85 000–140 000 g mol⁻¹), PCBM (MW = 910.9 g mol⁻¹) and ITO transparent electrode were obtained from Aldrich Chemical Company, Solenne, bv, Sigma Corp. and Präzisions Glas & Optik GmbH, Germany, respectively. Air-stable n-type semiconductor PBI was synthesized according to the approach reported by Würthner and Kaiser.^[38]

Sample Preparation: Firstly, PVA with concentrations of 10 wt% were dissolved in 80 °C double-distilled water. The nonpolar reactant PCBM (4 mg mL⁻¹) and polar reactant PBI (20 mg mL⁻¹) were dispersed in non-polar solvent cyclohexanone and polar solvent thiophene, respectively. For reference experiment, half concentration of PCBM (2 mg mL⁻¹) was used. Secondly, each component was successively LBL spin-coated onto the cleaned ITO electrode at spin rate of 1500–2000 rpm for 2 min. Particularly, each deposited layer was dried immediately in an oven (60 °C for 30 min) and then coated by subsequent layer. Thirdly, the fabricated trilayer was heated in an oven (60 °C for 30 min) and then covered by another ITO electrode in a way that the upper and down electrode glasses were agglutinated without any contamination to the electrode and sample. Finally, after 12 h drying, the trilayer n-n heterojunction was reserved at room temperature in air for 3 months.

Sample Scaling: The thickness of PVA layer (d_{PVA}) was calculated according to $d_{\text{PVA}} = \epsilon_0 \epsilon_r S / C$, where the permittivity of vacuum $\epsilon_0 = 8.85 \times 10^{-12}$ (C² N⁻¹ m⁻²), the relative permittivity of PVA $\epsilon_r \approx 7.8$ –8, the active surface area $S = 2 \text{ mm} \times 2 \text{ mm}$ and the capacitance C was detected by MIC-4970D LCR Meter. The thickness of PCBM and PBI were directly measured by AFM.

Optoelectronic Experimental Apparatus: Optoelectronic experiments were carried out by a home-built optoelectronic setup, constituted by a 532 nm wavelength green light source (continuous laser, compass 315M-100) with laser intensity of 99 mW cm⁻² if

not specified, a DC source (Keithley 617 electrometer), a sensitive galvanometer (Keithley 6485 picoammeter) in series with a resistance ($R = 10^4$ – $10^5 \Omega$), a program-controlled chopper for the temporal control for switching the laser on and off, a lens for adjusting laser beam width, and a coherent field master power meter for estimating the laser intensity (SI, Figure S3).

Supporting Information

Supporting Information is available from the Wiley Online Library or from the author.

Acknowledgements

This work is funded by SFB Transregio TRR 61 “Multilevel Molecular Assemblies”A6. J.L. is grateful to Prof. K. Huber (Uni. Paderborn, Germany), Prof. L. F. Chi, and Dr. L. Q. Li (AG Fuchs, Uni. Münster, Germany) for stimulating discussions, and also acknowledge to the support of Hubei Natural Science Foundation (Grant no. HNSF 2009CDA030).

This Communication is part of the Special Issue on Multilevel Molecular Assemblies: Structure, Dynamics, and Functions—a project of the Transregional Collaborative Research Center (TRR 61).

- [1] A. I. Gubanov, *Zh. Tekh. Fiz.* **1951**, 21, 304.
- [2] a) Ch. Kittel, *Einführung in die Festkörperphysik*, 14. Aufl., Oldenbourg Verlag, München/Wien **2006**; b) S. K. Islam, F. C. Jain, G. Zhao, E. Heller, *J. Infrared Milli. Terahz. Waves* **1998**, 19, 1633.
- [3] D. Yan, H. Wang, B. Du, *Introduction to Organic Semiconductor Heterojunctions*, John Wiley & Sons (Asia) Pty. Ltd., Singapore **2010**.

- [4] J. C. Scott, *J. Vac. Sci. Technol. A* **2003**, *21*, 521.
- [5] D. J. Yun, D.-K. Lee, H.-K. Jeon, S.-W. Rhee, *Org. Electron.* **2007**, *8*, 690.
- [6] N. S. Sariciftci, L. Smilowitz, A. J. Heeger, F. Wudi, *Science* **1992**, *258*, 1474.
- [7] A. Franciosi, C. G. Van de Walle, *Surf. Sci. Rep.* **1996**, *25*, 1.
- [8] J. Simon, V. Protasenko, C. Lian, H. Xing, D. Jena, *Science* **2009**, *327*, 60.
- [9] J. J. Benson-Smith, H. Ohkita, S. Cook, J. R. Durrant, D. D. C. Bradley, J. Nelson, *Dalton Trans.* **2009**, 10000.
- [10] E. J. Meijer, D. M. de Leeuw, S. Setayesh, E. Van Veenendaal, B.-H. Huisman, P. W. M. Blom, J. C. Hummelen, U. Scherf, T. M. Klapwijk, *Nat. Mater.* **2003**, *2*, 678.
- [11] a) T. D. Anthopoulos, C. Tanase, S. Setayesh, E. J. Meijer, J. C. Hummelen, P. W. M. Blom, D. M. de Leeuw, *Adv. Mater.* **2004**, *16*, 2174; b) T. D. Anthopoulos, D. M. de Leeuw, E. Cantatore, S. Setayesh, E. J. Meijer, C. Tanase, J. C. Hummelen, P. W. M. Blom, *App. Phys. Lett.* **2004**, *85*, 4205.
- [12] J. Kanicki, in *Handbook of Conducting Polymers* (Ed.: T. A. Skotheim), Dekker, New York **1986**.
- [13] W. G. Oldham, A. G. Milnes, *Solid-State Electron.* **1963**, *6*, 121.
- [14] N. Karl, *Defect Control in Semiconductors* (Ed.: K. Sumino), Vol. 2, Elsevier Science Publishers B. V., Noth-Holland, Amsterdam **1990**.
- [15] H. Dong, C. Wang, W. Hu, *Chem. Commun.* **2010**, *46*, 5211.
- [16] a) H. Qian, F. Negri, C. Wang, Z. Wang, *J. Am. Chem. Soc.* **2008**, *130*, 17970; b) M. A. Ibrahim, H.-K. Roth, U. Zhokhavets, G. Gobsch, S. Sensfuss, *Sol. Energy Mater. Sol. Cells* **2005**, *85*, 13.
- [17] a) F. Capasso, G. Margaritondo, *Heterojunction Band Discontinuities: Physics and Device Applications*, Elsevier Science Ltd., North-Holland, Amsterdam **1987**; b) A. Muoz, N. Chetty, Richard M. Martin, *Phys. Rev. B* **1990**, *41*, 2976.
- [18] a) F. Capasso, A. Y. Cho, K. Mohammed, P. W. Foy, *Appl. Phys. Lett.* **1985**, *46*, 664; b) F. Capasso, K. Mohammed, A. Y. Cho, *J. Vac. Sci. Technol. B* **1985**, *3*, 1245; c) F. Capasso, *Science* **1987**, *235*, 172.
- [19] C. G. van de Walle, R. M. Martin, *Phys. Rev. B.* **1987**, *35*, 8154.
- [20] a) H. Matsuura, *New J. Phys.* **2000**, *2*, 8.1; b) A. Horn, O. Katz, G. Bahir, J. Salzman, *Semicond. Sci. Technol.* **2006**, *21*, 933; c) C. Wood, D. Jena, *Polarization Effects in Semiconductors: From Ab Initio Theory to Device Applications*, Springer-Verlag, Berlin **2008**.
- [21] a) M. G. Helander, Z. B. Wang, J. Qiu, Z. H. Lub, *Appl. Phys. Lett.* **2008**, *93*, 193310; b) G. Hirankumar, S. Selvasekarapandian, N. Kuwata, J. Kawamura, T. Hattori, *J. Power Sources* **2005**, *144*, 262.
- [22] a) İ. Taşçioğlu, U. Aydemir, Ş. Altındal, B. Kınacı, S. Özçelik, *J. Appl. Phys.* **2011**, *109*, 054502; b) T. G. Abdel-Malik, R. M. Abdel-Latif, A. Sawaby, S. M. Ahmed, *J. Appl. Sci. Res.* **2008**, *4*, 331.
- [23] S. Kulanthaisami, D. Mangalaraj, K. Narayandass, *Eur. Polym. J.* **1995**, *31*, 969.
- [24] a) F. H. Abd El-Kader, G. Attia, S. S. Ibrahim, *J. Polym. Degrad. Stab.* **1994**, *43*, 253; b) X. Lu, N. Brown, M. Shaker, I. L. Kamel, *J. Polym. Sci. Part B* **1995**, *33*, 153; c) Y. Tanaka, Y. Mita, Y. Ohki, H. Yoshioka, M. Ikeda, F. Yazaki, *J. Phys. D* **1990**, *23*, 1491; d) F. H. Abd El-kader, S. S. Hamza, G. Attia, *J. Mater. Sci.* **1993**, *28*, 6719.
- [25] a) H. M. Zidan, *J. Appl. Polym. Sci.* **2003**, *88*, 516; b) G. V. Kumara, R. Chandramani, *App. Surf. Sci.* **2009**, *255*, 7047; c) B. Chandar Shekar, V. Veeravazhuthi, S. Sakthivel, D. Mangalaraj, K. Narayandass, *Thin Solid Films* **1999**, *348*, 122.
- [26] Th. B. Singh, N. Marjanović, G. J. Matt, N. S. Sariciftci, R. Schwödiauer, S. Bauer, *Appl. Phys. Lett.* **2004**, *85*, 5409.
- [27] T. P. Nguyen, C. Renaud, P. L. Rendu, S. H. Yang, *Phys. Status Solidi. C* **2009**, *6*, 1856.
- [28] Y. S. Yang, T. Zyung, *Macromol. Res.* **2002**, *10*, 75.
- [29] M. Pavlović, B. Šantić, D. I. Desnica-Frankoć, N. Radić, T. Šmuc, U. V. Desnica, *J. Electron. Mater.* **2003**, *32*, 1100.
- [30] a) G. Paradossi, F. Cavaliere, E. Chiessi, V. Ponassi, V. Martorana, *Biomacromolecules* **2002**, *3*, 1255; b) T. -S. Tsai, V. Pillay, Y.-E. Choonara, L. C. du Toit, G. Modi, D. Naidoo, P. Kumar, *Polymers* **2011**, *3*, 150.
- [31] Z. Rivera-Alvarez, L. Hernández, M. Becerrilla, A. Picos-Vega, O. Zelaya- Angel, R. Ramírez-Bon, J. R. Vargas-García, *Solid State Commun.* **2000**, *113*, 621.
- [32] A. Thander, B. Mallik, *Solid. State Commun.* **2002**, 159.
- [33] P. Chang, Y.-S. Lin, *Appl. Phys. Lett.* **2001**, *79*, 3666.
- [34] D. S. Jeong, C. S. Hwang, *J. App. Phys.* **2005**, *98*, 113701.
- [35] a) S.-K. Jeong, Y.-K. Jo, N.-J. Jo, *Electrochim. Acta.* **2006**, *52*, 1594; b) M. Z. Kufian, S. R. Majid, A. K. Arof, *Ionics* **2007**, *13*, 231.
- [36] J. L. Bredas, J. R. Durrant, *Acc. Chem. Res.* **2009**, *42*, 1689.
- [37] K.-J. Baeg, Y.-Y. Noh, J. Ghim, B. Lim, D.-Y. Kim, *Adv. Funct. Mater.* **2008**, *18*, 3678.
- [38] a) S. F. Würthner, A. Sautter, J. Schilling, *J. Org. Chem.* **2002**, *67*, 3037; b) T. E. Kaiser, V. Stepanenko, F. Würthner, *J. Am. Chem. Soc.* **2009**, *131*, 6719.

Received: August 30, 2011
Published online: